1 **Shifting microbial communities sustain multi-year iron reduction and methanogenesis in**

2 **ferruginous sediment incubations**

3 Marcus S. Bray[1], Jieying Wu[1], Benjamin C. Reed[1], Cecilia B. Kretz[2], Rachel L. Simister[3],

4 Cynthia Henny[4], Frank J. Stewart[1,2], Thomas J. DiChristina[1,2], Jay A. Brandes[5], David A.

5 Fowle[6], Sean A. Crowe[3], Jennifer B. Glass[1,2#]

6 [1]School of Biology, Georgia Institute of Technology, Atlanta, GA, 30332, USA

7 [2]School of Earth and Atmospheric Sciences, Georgia Institute of Technology, Atlanta, GA,

8 30332, USA

9 [3]Departments of Microbiology & Immunology and Earth, Ocean, & Atmospheric Sciences,

10 University of British Columbia, Vancouver, BC, Canada

11 [4]Research Center for Limnology, Indonesian Institute of Sciences, Cibinong, Indonesia

12 [5]Skidaway Institute of Oceanography, Savannah, GA, 31411, USA

13 [6]Department of Geology, University of Kansas, Lawrence, KS, 66045, USA

14 [#]Correspondence: 311 Ferst Drive Atlanta, GA; Telephone: 404-894-3942; Fax: 404-894-5638;

15 Email: Jennifer.Glass@eas.gatech.edu

16

17 Type: Research Article

18

Abstract

Reactive Fe^{3+} minerals can influence methane (CH_4) emissions by inhibiting microbial methanogenesis or by stimulating anaerobic CH_4 oxidation. The balance between Fe^{3+} reduction, methanogenesis, and methane oxidation in the ferruginous Archean oceans would have controlled CH_4 fluxes to the atmosphere, thereby regulating the capacity for CH_4 to warm the early Earth under the Faint Young Sun. We studied CH_4 and Fe cycling in anoxic incubations of ferruginous sediment from the Archean ocean analogue Lake Matano, Indonesia over three successive transfers (500 days total). Iron reduction, methanogenesis, methane oxidation, and microbial taxonomy were monitored in treatments amended with 10 mM ferrihydrite or goethite. After three dilutions, Fe^{3+} reduction persisted only in bottles with ferrihydrite. Enhanced CH_4 production was observed in the presence of goethite. Methane oxidation was observed throughout incubations, although stoichiometry suggested that Fe^{3+} was not the sole electron acceptor. 16S rRNA profiles continuously changed over the course of enrichment, with ultimate dominance of unclassified members of the order Desulfuromonadales in all treatments and Rhodocyclaceae in treatments amended with CH_4. Microbial diversity decreased markedly over the course of incubation, with subtle differences being observed between ferrihydrite and goethite. These results suggest that Fe^{3+}-oxide mineralogy and availability of electron donors could have led to spatial separation of Fe^{3+}-reducing and methanogenic microbial communities in ancient ferruginous marine sediments, potentially explaining the persistence of CH_4 as a greenhouse gas throughout the Archean.

41   **INTRODUCTION**

42   Anoxic and ferruginous conditions were common in Archean oceans (Poulton & Canfield, 2011).

43   In Archean seawater, Fe would have undergone extensive redox cycling via microbial

44   photoferrotrophy or abiotic photo-oxidation of dissolved Fe^{2+} to Fe^{3+} followed by microbial

45   respiration of Fe^{3+} to Fe^{2+} (Kappler et al., 2005 ; Crowe et al., 2008a ; Konhauser et al., 2005).

46   Indeed, Fe^{3+} reduction evolved early in Earth's history (Craddock & Dauphas, 2011 ; Johnson et

47   al., 2008) and may have contributed extensively to organic matter oxidation in the Archean

48   (Vargas et al., 1998).

49   Elevated atmospheric methane (CH_4; 100-1000 ppmv in the Archean vs. ~2 ppmv in the

50   modern atmosphere) could have played a role in the Archean greenhouse effect that sustained

51   temperatures warm enough for liquid water under considerably lower solar radiation (Pavlov et

52   al., 2000 ; Haqq-Misra et al., 2008 ; Kasting, 2005). The source of Archean CH_4 was likely

53   hydrogenotrophic methanogenesis ($CO_2 + 4\ H_2 \rightarrow CH_4 + 2H_2O$; (Ueno et al., 2006 ; Battistuzzi

54   et al., 2004). However, this form of methanogenesis typically yields minimal free energy and is

55   outcompeted by metal-reducing organisms with a higher affinity for H_2 than methanogens in the

56   presence of poorly crystalline Fe^{3+} (e.g. ferrihydrite; Lovley & Phillips, 1987 ; Lovley &

57   Goodwin, 1988 ; Zhou et al., 2014). Ferrihydrite reduction can also outcompete acetoclastic

58   methanogenesis ($CH_3COO^- + H^+ \rightarrow CH_4 + CO_2$) due to the higher affinity for acetate (CH_3COO^-

59   ) by Fe^{3+}-reducing bacteria compared to methanogens (Lovley & Phillips, 1986), although

60   acetoclastic methanogenesis likely evolved late in Earth's history (Fournier & Gogarten, 2008).

61   Ferruginous oceans would have further suppressed CH_4 emissions if Fe^{3+} played a role in

62   supplying electron acceptors for CH_4 oxidation, either as the direct oxidant, or indirectly through

63   the regeneration of sulfate through oxidation of reduced sulfur compounds (Sivan et al., 2014).

64   Methane oxidation coupled directly to Fe^{3+} reduction is thermodynamically favorable

65   according to the free energy yield with ferrihydrite ($CH_4 + 8\ Fe(OH)_3 + 15H^+ \rightarrow HCO_3^- + 8Fe^{2+}$

66    $+ 21H_2O$; ΔG_r^0 = -571 kJ mol^{-1} CH_4) and goethite ($CH_4 + 8\ FeOOH + 15H^+ \rightarrow HCO_3^- + 8Fe^{2+} +$

67    $13H_2O$; ΔG_r^0 = -355 kJ mol^{-1} CH_4) as terminal electron acceptors. We would expect to observe a

68   stoichiometric ratio of 1 CH_4 oxidized per 8 Fe^{3+} reduced and, based on energetic yields, the

69   preferential use of ferrihydrite over goethite as the electron acceptor in this putative metabolism.

70   In addition, accumulating geochemical evidence for microbial CH_4 oxidation coupled to, or

71   stimulated by, Fe^{3+} reduction is widespread across modern anoxic ecosystems and anaerobic

72   digester communities (Sivan et al., 2011 ; Segarra et al., 2013 ; Beal et al., 2009 ; Amos et al.,

73   2012 ; Riedinger et al., 2014 ; Noroi et al., 2013 ; Crowe et al., 2011 ; Sturm et al., 2015 ;

74   Egger et al., 2015 ; Zehnder & Brock, 1980 ; Sivan et al., 2014 ; Fu et al., 2016 ; Rooze et al.,

75   2016). However, robust and direct evidence for this putative metabolism in the form of stable

76   enrichment cultures or microbial isolates remains elusive.

77   Despite the possible importance of coupled Fe and CH_4 cycling in the Archean Eon,

78   long-term studies of Fe^{3+} reduction under low organic carbon and high CH_4 conditions remain

79   sparse. Lake Matano, Indonesia is one of the only modern analogues for the ferruginous Archean

80   oceans (Crowe et al., 2008a). Despite the presence of Fe^{3+} oxides that might be expected to

81   suppress methanogenesis, CH_4 accumulates to 1.4 mM in anoxic deep waters (Crowe et al.,

82   2008a ; Crowe et al., 2011 ; Crowe et al., 2008b ; Crowe et al., 2007). Methanotrophy is a key

83   carbon fixation process in Lake Matano's oxic-anoxic transition zone, and the dearth of other

84   oxidants (<100 nM nitrate and sulfate) suggests that Fe^{3+} might be the primary electron acceptor

85   in methanotrophy (Sturm et al., 2015 ; Crowe et al., 2011). In this study, we examined the

86   influence of CH_4 and Fe^{3+} mineral speciation on CH_4 and Fe biogeochemistry together with

87   microbial community composition over three successive dilutions (500 total days of incubation)

88   of anoxic Lake Matano sediments.

89

90   **MATERIALS AND METHODS**

91

92   **Sample collection and storage**

93   A 15-cm sediment core from 200 m water depth in Lake Matano, Sulawesi Island, Indonesia

94   (2°26′S, 121°15′E; *in situ* sediment temperature ~27°C) was sampled in November 2010 and

95   sub-sampled at 5 cm increments. Sediments from 0-5 and 5-10 cm depth were fluffy and black,

96   and 10-15 cm was dark gray. Sediments were sealed in gas-tight bags with no headspace

97   (Hansen et al., 2000) and stored at 4°C until incubations began in March 2015.

98

99   **Enrichment medium and substrate synthesis**

100   A modified artificial freshwater medium lacking nitrate and sulfate was developed based on the

101   pore water composition of Lake Matano sediments (S.A. Crowe and D.A. Fowle, unpublished

102   work). The medium contained 825 μM $MgCl_2$, 550 μM $CaCO_3$, 3 mM $NaHCO_3$, 3.5 μM

103   K_2HPO_4, 5 μM Na_2HPO_4, 225 μM NH_4Cl, 1 μM $CuCl_2$, 1.5 μM Na_2MoO_4, 2.5 μM $CoCl_2$, 23

104   μM $MnCl_2$, 4 μM $ZnCl_2$, 9.4 μM $FeCl_3$ and 3 mM Na_2NTA, 0.07 μM vitamin B_{12}, 0.4 μM biotin,

105   and 68.5 μM thiamine. Filter-sterilized vitamin solutions were added after autoclaving.

106   Ferrihydrite ($Fe(OH)_3$) and goethite (FeOOH) were synthesized as described in Schwertmann &

107   Cornell (1991) and added to enrichments to 10 mM as described below.

108

109   **Inoculation of enrichment and amendments**

5

110   The sediment was pre-treated for 36 days at 30°C in 100% N_2 headspace to deplete endogenous

111   organic carbon, electron donors, and reactive electron acceptors. After pre-treatment, sediment

112   from the 0-5 cm depth layer was inoculated in a ratio of sediment to medium of 1:5 (v/v) in an

113   anoxic chamber (97% N_2 and 3% H_2; Coy Laboratory Products, Grass Lake, MI, USA).

114   Sediment slurry (35 mL) was aliquoted into 70 mL sterile serum bottles, stoppered with sterile

115   butyl stoppers (Geo-Microbial Technologies, Ochelata, OK, USA; pre-boiled in 0.1 N NaOH),

116   and crimped with aluminum seals. Ferric iron was added either as ferrihydrite or goethite to 10

117   mM. Bottles were purged with 99.99% N_2 for 1 hr, and CH_4 amendments were injected with 10

118   mL 99.99% CH_4 and 5 mL 99% $^{13}CH_4$ (Cambridge Isotope Laboratories, Tewksbury, MA,

119   USA). Controls were autoclaved at 121°C for 1 hr on day 0 and again on day 6 of the 1°

120   enrichment. All treatments were duplicated, and bottles were incubated in the dark at 30°C with

121   shaking at 200 rpm.

122   After 50 days, the volume of all cultures was reduced to 5 mL, and 30 mL of fresh media

123   was added to each bottle, constituting a 6-fold dilution. These 2° enrichments were amended

124   with an additional 10 mM of either ferrihydrite or goethite. All bottles were purged with 99.99%

125   N_2 for 1 hr, and all bottles except N_2 controls were injected with 8 mL 99.99% CH_4 and 2 mL

126   99% $^{13}CH_4$. Controls were autoclaved again at 121°C for 1 hr. DL-Methionine (10 µM) was

127   added as a sulfur source. After 303 days, cultures were diluted 10-fold with fresh media into new

128   serum bottles (3° enrichment) with the same substrate and headspace composition as the 2°

129   enrichment. A schematic of the incubation and dilutions is shown at the top of Figures 1-3.

130

131   **HCl-extractable Fe^{2+} and Fe^{3+} and soluble Fe^{2+}**

132   Samples were taken from each bottle in the anoxic chamber using a 22-gauge needle and plastic

133   syringe. Plasticware was stored in the anoxic chamber for at least 24 hr to minimize O_2 sample

134   contamination. For HCl-extractable Fe^{2+} analyses, 100 µL of sediment slurry was extracted with

135   400 µL 0.5 N HCl in the dark for 1 hr, followed by centrifugation at 10,000 x g for 1 min,

136   injection of 10 µL of supernatant into 990 µL of 10 mM FerroZine reagent in 46 mM HEPES

137   (pH 8.3), and measurement of absorbance at 562 nm (Stookey, 1970). For HCl-extractable Fe^{3+},

138   100 µL of sediment slurry was incubated overnight in 0.5 N HCl and 0.25 M NH_2OH-HCl in the

139   dark, followed by centrifugation and measurement as above, and subtraction of HCl-extractable

140   Fe^{2+} as in Kostka & Luther (1994).

141

142   **Methane oxidation**

143   Samples were collected for δ^{13}C-DIC analysis by 0.2 µm membrane filtration of medium into

144   crimp top autosampler vials (Thermo Scientific National Target LoVial) and analysis as

145   described in Brandes (2009). Rates of $^{13}CH_4$ oxidation to ^{13}C-DIC were calculated over the linear

146   period of δ^{13}C-DIC increase based on the method in Scheller et al. (2016). First, the δ^{13}C-DIC

147   values were converted into fractional abundances ($^{13}F = (^{13}C/^{12}C+^{13}C)$), and then DIC production

148   from CH_4 oxidation was calculated using the following formula:

149                          $\Delta[\text{DIC}] = ([\text{DIC}]_n(^{13}F_n)) - ([\text{DIC}]_0(13F_0))/^{13}F_{CH4}$

150   Where $[\text{DIC}]_n$ and $^{13}F_n$ are equal to the total DIC concentration (mM) and fractional abundance

151   of ^{13}C in the DIC at time n respectively. $[\text{DIC}]_0$ and $^{13}F_0$ are the total DIC concentration (mM)

152   and fractional abundance of DIC at time 0 respectively, and $^{13}F_{CH4}$ is the fractional abundance of

153   ^{13}C in the CH_4.

154

155 **Methane in headspace**

156 Headspace (50 µL) was sampled using a gastight syringe and injected into a gas chromatograph

157 (SRI Instruments 8610C, Torrance, CA, USA) with a HayeSep N column and flame ionization

158 detector to measure headspace CH_4 concentrations. A CH_4 standard (1000 ppm, Airgas, USA)

159 was used for calibration.

160

161 **16S rRNA gene amplicon sequencing**

162 Samples (2 mL) of sediment used for inoculating incubations (hereafter, "sediment inoculum")

163 were taken in February 2015 (prior to pre-treatment) and after incubation for 15 days (1°

164 enrichment), 72 days (2° enrichment) and 469 days (3° enrichment). Nucleic acid was extracted

165 and purified using a PowerSoil Isolation Kit following the manufacturer's protocol (Catalog #

166 12888; MO BIO, Carlsbad, CA, USA) and UltraClean® 15 Purification Kit (MO BIO

167 Laboratories, Carlsbad, CA). 16S rRNA gene amplicons were synthesized from extracted DNA

168 with V4 region-specific barcoded primers F515 and R806 (Caporaso et al., 2011) appended with

169 Illumina-specific adapters according to Kozich et al. (2013) using a C1000 Touch Thermocycler

170 (Bio-Rad, Hercules, CA) and QIAGEN Taq PCR Master Mix (QIAGEN, Venlo, Netherlands).

171 Thermal cycling conditions were as follows: initial denaturing at 94°C (5 min), 35 cycles of

172 denaturing at 94°C (40 sec), primer annealing at 55°C (40 sec), and primer extension at 68°C (30

173 sec). Amplicons were checked for correct size (~400 bp) on a 1% agarose gel and purified using

174 Diffinity RapidTips (Diffinity Genomics, West Henrietta, NY, USA). Amplicon concentrations

175 were determined fluorometrically on a Qubit[TM] (ThermoFisher Scientific, Waltham,

176 Massachusetts, USA). Amplicons were pooled at equimolar concentrations (4 nmol), and

177 sequenced on an Illumina MiSeq running MiSeq Control software v.2.4.0.4 using a 500 cycle

178   MiSeq reagent kit v2 with a 5% PhiX genomic library control, as described by Kozich et al.

179   (2013). Sequences were deposited as NCBI accession numbers SAMN04532568-04532641 and

180   SAMN05915184-05915222.

181

182   **16S rRNA gene amplicon sequence analysis**

183   Demultiplexed amplicon read pairs were quality trimmed with Trim Galore (Babraham

184   Bioinformatics) using a base Phred33 score threshold of Q25 and a minimum length cutoff of

185   100 bp. Reads were then analyzed using mothur (Schloss et al., 2009) following its MiSeq

186   standard operating procedure. High quality paired reads were merged and screened to remove

187   sequences of incorrect length and those with high numbers of ambiguous base calls. Merged

188   reads were dereplicated and aligned to the ARB SILVA database (release 123; available at

189   http://www.mothur.org/wiki/Silva_reference_alignment). Sequences with incorrect alignment

190   and those with homopolymers longer than 8bp were filtered out. Unique sequences and their

191   frequency in each sample were identified and then a pre-clustering algorithm was used to further

192   de-noise sequences within each sample. Sequences were then chimera checked using UCHIME

193   (Edgar et al., 2011). Reads were then clustered into OTUs at 97% similarity based on

194   uncorrected pairwise distance matrices. OTUs were classified using SILVA reference taxonomy

195   database (release 123, available at http://www.mothur.org/wiki/Silva_reference_files). Chao 1

196   (species richness), phylogenetic diversity, and Shannon index (species evenness) estimates were

197   generated using mother after normalization to 4000 sequences per sample.

198

199   **RESULTS**

200   **Iron reduction**

201 *1° enrichment*. Over the first 10 days of incubation, HCl-extractable Fe^{2+} increased from 10 to 25

202 mM in ferrihydrite treatments (Fig. 1a) and from 10 to 20 mM in goethite treatments (Fig. 1b).

203 From day 6 to 10, HCl-extractable Fe^{3+} (7 and 12 mM in ferrihydrite and goethite treatments,

204 respectively) was completely consumed in all bottles except autoclaved controls with ferrihydrite

205 (data not shown). Iron reduction rates were identical with and without CH_4 (Fig. 1a, b). Initial

206 autoclaving did not suppress Fe^{3+} reduction. A second round of autoclaving on day 6 slightly

207 suppressed further activity. From day 10-28, HCl-extractable Fe^{2+} fluctuated in ferrihydrite

208 treatments (Fig. 1a) and declined slightly in goethite treatments (Fig. 1b). Soluble Fe^{2+} was

209 consistently <1% of HCl-extractable Fe^{2+}, and sediment-free controls did not reduce Fe^{3+} (data

210 not shown).

211 *2° enrichment*. After 1:6 dilution and 10 mM ferrihydrite addition on day 50, HCl-extractable

212 Fe^{2+} increased from 3 to 4 mM over the first two days, and then remained constant through the

213 final time point (day 497) in bottles with and without added CH_4 (Fig. 1a). After 10 mM goethite

214 addition on day 50, HCl-extractable Fe^{2+} increased from 2 to 3 mM after a two-day lag period.

215 Thereafter, HCl-extractable Fe^{2+} rose to 4 mM by day 497 in goethite treatments with added

216 CH_4; without CH_4, HCl-extractable Fe^{2+} dropped back to 2 mM (Fig. 1b). Autoclaved controls

217 had no activity. Black magnetic minerals formed in all ferrihydrite treatments except autoclaved

218 controls (Fig 1a). No magnetic minerals formed in goethite treatments (Fig. 1b).

219 *3° enrichment*. After 1:10 dilution and addition of 10 mM ferrihydrite on day 352, HCl-

220 extractable Fe^{2+} doubled in the first week in N_2 treatments and bottle CH_4-1 (Fig. 1a). Bottle

221 CH_4-2 displayed similar activity after a two-week lag period. After an additional 100 days, HCl-

222 extractable Fe^{2+} had increased to 2 mM in CH_4 treatments and 1 mM in the N_2 treatment by day

223 466. Goethite treatments had minimal activity after the first week of 3° enrichment (Fig. 1b).

224   Autoclaved controls had no activity. As in the 2° enrichment, magnetic minerals formed in the

225   presence of ferrihydrite (Fig. 1a), but not goethite (Fig. 1b).

226

Methane production

228   Goethite treatments consistently displayed higher CH_4 production than those with ferrihydrite

229   (Fig. 2). Methanogenesis started during the initial period of Fe^{3+} reduction, and stopped after

230   HCl-extractable Fe^{3+} was completely consumed in the 1° enrichment (day 10). Methanogenesis

231   continued throughout the 3° enrichment. Negligible CH_4 was produced in treatments with

232   ferrihydrite, except for bottle N_2-2 in the 3° enrichment.

233

Methane oxidation

235   *1° enrichment.* ^{13}C incorporation into DIC began on day 6 in both ferrihydrite and goethite

236   treatments and continued throughout the 1° enrichment (Fig. 3a,b). Ferrihydrite treatments

237   showed lower ^{13}C enrichment of the DIC pool but higher total DIC production (totaling to 1.7

238   and 1.1 µM CH_4 d^{-1} for bottles 1 and 2, respectively) than goethite treatments, which had greatest

239   $\delta^{13}C$ enrichment, but minimal DIC production (0.2 and 0.8 µM CH_4 d^{-1} for bottles 1 and 2,

240   respectively). Autoclaved controls showed neither ^{13}C incorporation nor DIC production.

241   *2° enrichment.* Both ferrihydrite treatments displayed ^{13}C enrichment (Fig. 3a), but declined in

242   DIC, precluding calculation of CH_4 oxidation rates. Initial pH of 8 declined to 7.6, 6.7 and 6 in

243   the autoclaved, N_2 and CH_4 treatments, respectively. DIC in goethite treatments with CH_4

244   dropped to undetectable values within three weeks, suggesting sampling or analytical error,

245   which precluded accurate isotopic measurement at these time points. These data are thus not

246   considered further. Autoclaved and N_2 controls did not show pH changes.

247   *3° enrichment*. Bottle CH_4-2 with ferrihydrite was the only treatment with significant ^{13}C

248   incorporation into DIC over the first 15 days (Fig. 3a). DIC also increased over the same interval

249   in both ferrihydrite-amended bottles; calculated CH_4 oxidation rates were 32 and 7 $\mu M\ d^{-1}$ in

250   bottle 1 and 2, respectively. The pH dropped from 8.2 to 7.1 and 7.9 in bottles 1 and 2,

251   respectively, over the first 15 days. By day 470, ^{13}C enrichment and DIC concentrations in both

252   ferrihydrite-amended bottles had returned to a level similar to that at the start of the 3°

253   enrichment. Autoclaved controls did not exhibit any change in DIC and pH. Goethite treatments

254   had initial DIC concentrations (3-5 mM) higher than those in previous enrichments. In the

255   goethite-amended autoclaved controls and bottle CH_4-1, DIC concentrations dropped over the 3°

256   enrichment. Only goethite-amended bottle CH_4-2 increased in DIC, without concurrent ^{13}C

257   enrichment.

258

Microbial taxonomy

260   *Inoculum*. 16S rRNA gene amplicons from the sediment inoculum were dominated by those

261   classified as Bathyarchaeota (25%), formerly Miscellaneous Crenarchaeotal Group (MCG; Fig.

262   4) and unclassified Archaea (11%).

263   *1° enrichment*. After 15 days of incubation with Fe^{3+} substrates, species, richness, evenness and

264   phylogenetic diversity decreased relative to the inoculum in all treatments (Fig. 4).

265   Geobacteraceae (Deltaproteobacteria) became dominant (22-36%) in all ferrihydrite treatments

266   (Fig. 4a); the dominant OTU had 97% similarity to *Geothermobacter* sp. Ferrihydrite-amended

267   bottle CH_4-1 was enriched in the Betaproteobacteria, specifically Comamonaceadeae (17%) and

268   Rhodocyclaceae (9%; Fig. 4a). Bathyarchaeota persisted in goethite treatments (11-25%; Fig.

269   4b).

270   *2° enrichment*. By day 72, all treatments had lower species richness, phylogenetic diversity, and

271   evenness. Unclassified Desulfuromondales dominated both ferrihydrite and goethite enrichments

272   (34-68% and 39-53% with ferrihydrite and goethite, respectively). The dominant OTU had 98%

273   similarity to *Geobacter hephaestius.* Bathyarchaeota were depleted compared to the 1°

274   enrichment (Fig. 4). Geobacteraceae declined in ferrihydrite enrichments (2-18%; Fig. 4a).

275   Campylobacteraceae (Epsilonproteobacteria), which was insignificant in the inoculum and the 1°

276   enrichment, comprised 23-40% of sequences in goethite treatments with CH_4; the dominant OTU

277   had 98% similarity to *Sulfurospirillum barnesii* (Fig. 4b). The most abundant methanogenic

278   Euryarchaeota order, Methanobacteriaceae, comprised 1-2% and 6-7% of sequences in

279   ferrihydrite and goethite treatments, respectively the dominant OTU has 100% similarity to

280   *Methanobacterium flexile*.

281   *3° enrichment*. By day 469, species richness, phylogenetic diversity, and evenness were even

282   lower than in the 2° enrichment (Fig. 4a,b). Unclassified Desulfuromondales dominated goethite

283   treatments (32-76%; Fig. 4b), but comprised only 18-38% of ferrihydrite treatments. The

284   dominant OTU also had 98% identity to *Geobacter hephaestius/lovleyi*, as in the 2° enrichment.

285   Rhodocyclaceae were more abundant in ferrihydrite treatments with CH_4 (14-15%) than with N_2

286   (2-4%; Fig 4a); the dominant OTU had 100% similarity to *Azospira oryzae/Dechlorosoma*

287   *suillum*. Peptococcaceae (Firmicutes) were most abundant in bottle CH_4-2 with ferrihydrite

288   (30%); the dominant OTU had 96% similarity to uncultured members of the genus *Thermincola*.

289   Syntrophaceae (Deltaproteobacteria) were enriched in all ferrihydrite treatments (11-16%) and

290   goethite treatments with N_2 (8-15%); the dominant OTU had 97% similarity to *Smithella*

291   *propionica*. Methanobacteriaceae comprised 1-4% of sequences in goethite treatments and were

292   absent from ferrihydrite treatments; as in the 2° enrichment, the dominant OTU had 100%

293   identity to *Methanobacterium flexile*.

294

295   **DISCUSSION**

296   **Rates of Fe^{3+} reduction in long-term ferruginous sediment incubations**

297   Initial rates of HCl-extractable Fe^{2+} production (~1-2 mM d^{-1}) in the 1° enrichment were similar

298   to those from freshwater wetlands (Roden & Wetzel, 2002 ; Jensen et al., 2003 ; Kostka et al.,

299   2002). Activity declined with each successive transfer (0.4 and 0.08 mM d^{-1} for 2° and 3°

300   enrichments, respectively), despite replenishment of Fe^{3+} substrates. Declining Fe^{3+} reduction

301   rates through the incubation period likely reflects limitation by availability of organic carbon, the

302   most thermodynamically favorable electron donor, which was diluted during each successive

303   transfer of the lake sediment. The next two most thermodynamically favorable electron donors

304   are H_2 and CH_4. Hydrogen could have been supplied by fermenters such as Syntrophaceae, but

305   would ultimately still require a source of organic carbon. Methane as an electron donor for

306   microbial Fe^{3+} reduction is thermodynamically favorable and coupling of Fe^{3+} reduction to CH_4

307   oxidation has been long suspected as a viable microbial metabolism (Caldwell et al., 2008 ;

308   Zehnder & Brock, 1980). In our 2° and 3° enrichments, CH_4 addition resulted in higher Fe^{2+}

309   yield with goethite and ferrihydrite, respectively. This could be the result of (a) methanotrophic

310   growth resulting in production of organics which is used by heterotrophic Fe^{3+} reducers or (b)

311   the direct coupling of CH_4 oxidation and Fe^{3+} reduction. No difference in initial Fe^{2+} production

312   rates however, suggests that initial CH_4 oxidation was driven by another electron donor.

313   Higher Fe^{3+} reduction rates were maintained on ferrihydrite than goethite, consistent with

314   the higher energetic yield of ferrihydrite vs. goethite as well as its typically greater surface-area.

14

315   Formation of magnetic minerals was likely due to adsorption of Fe^{2+} onto ferrihydrite followed

316   by solid-state conversion of ferrihydrite to magnetite (Hansel et al., 2003). Since the HCl-

317   extraction method does not dissolve magnetite and magnetite-adsorbed Fe^{2+} (Poulton & Canfield,

318   2005), it is possible that the Fe^{3+} reduction observed in the study is an underestimation of total

319   activity.

320

321 Fe^{3+} oxide mineralogy controls methane production and methanogen taxonomy

322   Our observation of higher rates of methanogenesis in goethite vs. ferrihydrite amendments is

323   consistent with prior results showing that bacteria that reduce ferrihydrite better outcompete

324   methanogenic archaea for H_2 and acetate than those that reduce goethite and other more

325   crystalline Fe^{3+} oxides (Lovley & Phillips, 1987 ; Lovley & Goodwin, 1988 ; Zhou et al., 2014 ;

326   Hori et al., 2010 ; Roden & Wetzel, 1996). This outcompetition is also broadly supported by

327   taxonomic shifts. In particular, anaerobic heterotrophs such as *Geothermobacter sp.* (Kashefi et

328   al., 2003) enriched in ferrihydrite treatments by day 15 may have outcompeted other microbes

329   for organic carbon sources.

330   Goethite treatments contained higher abundances of Methanobacteriaceae (0.1-1% and 1-

331   4% on days 15 and 469, respectively) than ferrihydrite treatments (≤0.1% throughout),

332   suggesting that CH_4 in goethite treatments came from the substrates used by

333   Methanobacteriaceae (H_2/CO_2, formate, or CO). The ferrihydrite treatment (bottle 2) that

334   produced CH_4 by day 469 contained 3% Methanosaetaceae, which produce CH_4 from acetate, or

335   from H_2/CO_2 via direct interspecies electron transfer with *Geobacter* (Rotaru et al., 2014). The

336   most dominant OTU had 98% similarity to *Methanosaeta concilii,* in agreement with

337   observations from the Lake Matano water column (Crowe et al., 2011). It is also possible that

338 archaea could be directly involved in Fe^{3+} reduction (Vargas et al., 1998 ; Sivan et al., 2016),

339 although the lack of methanogenesis in ferrihydrite treatments does not support this.

340

Fe^{3+}-dependent CH_4 oxidation

342 Enrichments were established under conditions thought favorable for Fe^{3+}-dependent CH_4

343 oxidation (e.g. Fe^{3+} oxides and CH_4 as the most abundant electron acceptors and donors,

344 respectively). Incorporation of $^{13}CH_4$ into DIC overlapped with the second phase of Fe^{3+}

345 reduction (days 6-10) in the 1° enrichment but continued after Fe^{3+} reduction stopped at day 10,

346 suggesting an alternative electron acceptor for CH_4 oxidation. Moreover, the stoichiometry of

347 CH_4 oxidized to Fe^{2+} reduced in the 1° enrichment was significantly lower than predicted (1:8;

348 Fig. 5). Low to negative rates of DIC production in the 2° enrichment complicated measurements

349 of CH_4 oxidation. In the 3° enrichment, significant DIC production and ^{13}C incorporation was

350 observed in the first 15 days in bottle CH_4-2 with ferrihydrite, but thereafter isotopic values

351 returned to background levels. The apparent spike in CH_4 oxidation was unlikely coupled to Fe^{3+}

352 reduction (Fig. 5). However, over the same time period, bottle CH_4-1 oxidized methane and

353 reduced iron in a ratio close to the 1 CH_4 oxidized: 8 Fe^{3+} reduced predicted for Fe-AOM (Fig.

354 5). Goethite-amended cultures were also close to the 1:8 line, albeit with extremely low CH_4

355 oxidation and Fe^{3+} reduction rates. By the end of 3° enrichment (day 466), CH_4-amended

356 treatments produced twice as much HCl-extractable Fe^{2+} as N_2 treatments, suggesting that Fe^{3+}

357 reduction was stimulated by CH_4. However, without evidence for CH_4 oxidation data during this

358 time interval, we cannot attribute this stimulation to Fe-AOM. It is important to note that these

359 CH_4 oxidation rates may be underestimates due to the low levels of DIC production in our

360 experiments. This suggests that high levels of autotrophy or CO_2 reduction to CH_4 may have

361   been taking place in our enrichments. In addition, decreasing pH values in some of our

362   enrichments could have pulled DIC into headspace CO_2 subsequently lowering DIC

363   concentrations.

364   Only minor community composition differences were observed between CH_4- and N_2-

365   cultures; by day 469, the only taxon that was more abundant in the CH_4 vs. N_2 treatments was the

366   betaproteobacterium *Azospira oryzae/Dechlorosoma suillum*, a member of the Rhodocyclaceae

367   family. The potential role of this microbe in CH_4 cycling remains unclear, as laboratory cultures

368   of this species are not known to oxidize CH_4. It is also possible that the growth of novel

369   organisms capable of high rates of Fe^{3+}-dependent CH_4 oxidation was inhibited by other

370   unidentified factors, potentially related to the batch-style incubations, the use of butyl rubber

371   stoppers (Niemann et al., 2015), or the lack of a critical substrate in the enrichment medium.

372

Effect of Fe^{3+} oxide and carbon substrates on microbial community diversity

374   The microbial community underwent multiple shifts over the 500-day incubation, with an overall

375   decrease in species richness, species evenness, and phylogenetic diversity over the course of

376   incubation. This was likely in response to declining organic carbon and alternative electron

377   donors. By the 3° enrichment, species evenness was consistently lower in each goethite-amended

378   treatment than in the respective ferrihydrite-amended treatment. This could mean that the greater

379   energetic yield of ferrihydrite reduction fosters higher diversity. Alternatively, the higher

380   reactivity of ferrihydrite may allow it to be utilized by more organisms than goethite.

381   All of the most enriched taxa have relatives that in laboratory cultures reduce Fe^{3+}.

382   Within those taxa, the most abundant OTUs were closely related to organisms capable of Fe^{3+}

383   reduction (*Geothermobacter sp.*, *Geobacter hephaestius/Geobacter lovleyi*, *Thermincola sp.*, and

17

384   *Sulfurospirillum barnesii*) (Kashefi et al., 2003 ; Zavarzina et al., 2007 ; Stolz et al., 1999). It is

385   important to note that all taxa enriched in our experiments comprised ≤0.1% of the inoculum

386   community. Desulfuromonadales was the only metal-reducing taxon that was continuously

387   present in all enrichments (3-11%, 34-53%, and 18-76% in the inoculum, 1°, 2°, and 3°

388   enrichment respectively). Other taxa significantly differed in their abundance over the course of

389   incubation. Geobacteraceae was enriched at day 15 with ferrihydrite (22-36%) but had declined

390   in abundance by day 72 (8-18%). Other taxa including Rhodocyclaceae and Peptocaccaceae,

391   were enriched in the presence of ferrihydrite at day 469. In goethite treatments,

392   Campylobacteraceae (23-40%) were enriched at day 72, but did not make up a significant

393   portion of the community at day 469. The succession of different metal-reducing taxa may be

394   due to the changing availability of electron donors (e.g. H_2 and organic C). Enrichment of

395   Syntrophaceae, known for their synthrophic fermentative interactions, suggests the establishment

396   of syntrophy in the 3° enrichment in response to depletion of electron donors.

397

Geobiological implications

399   The anaerobic microbial metabolisms studied here – Fe^{3+} reduction and hydrogenotrophic

400   methanogenesis – were likely of great importance to the Archean carbon cycle (Konhauser et al.,

401   2005 ; Posth et al., 2013 ; Johnson et al., 2008). The severe organic carbon limitation in our

402   incubations likely mimics conditions of the Archean ocean with relatively low amounts of

403   primary production and biopolymer degradation as well as the absence of complex organic

404   substances supplied by multicellular eukaryotes (Knoll et al., 2016 ; Farquhar et al., 2011). Our

405   results point to a mineralogical control on Fe^{3+}-reduction, methanogenesis, and microbial

406   community composition and diversity. Rapid sedimentation of amorphous Fe^{3+} phases like

18

407   ferrihydrite could have supported sediments with diverse communities of Fe^{3+}-reducing

408   organisms that could have outcompeted other taxa such as methanogens for limited carbon and

409   nutrients. Conversely, slow deposition and aging of ferrihydrite to goethite could have limited

410   both the abundance and diversity of Fe^{3+}-reducing organisms, allowing for the establishment of a

411   methanogenic community. Therefore, we posit that methanogenesis rates in the Archean would

412   have depended on the relative abundance of the Fe^{3+} phases and their distributions in marine

413   sediments. Sediments below shallow water columns were likely fed by abundant amorphous Fe^{3+}

414   from photoferrotrophic activity. In the open ocean, organic carbon and Fe^{3+} would have been

415   significantly consumed before reaching sediments, leaving only more crystalline iron phases that

416   are difficult to reduce. Importantly, the role of Fe^{3+}-driven CH_4 oxidation appears limited given

417   our experimental results, though we cannot rule out this pathway given that some of our data

418   suggest it may operate at low rates. Overall, our results support a model for an Archean

419   ferruginous biosphere supported by spatially segregated habitats of bacterial Fe^{3+} reduction from

420   reactive Fe^{3+} oxides, and archaeal methanogenesis in the presence of less reactive Fe^{3+} phases.

421   Rates of Fe deposition, aging, and recrystallization may thus have played an important role in

422   regulating the preservation of sedimentary Fe^{3+}, the production of methane, and the ecology and

423   diversity of the Archean biosphere.

424 **Acknowledgements**

References

Amos R, Bekins B, Cozzarelli I, Voytek M, Kirshtein J, Jones E, Blowes D (2012) Evidence for iron-mediated anaerobic methane oxidation in a crude oil-contaminated aquifer. *Geobiology,* **10**, 506-517.

Battistuzzi FU, Feijao A, Hedges SB (2004) A genomic timescale of prokaryote evolution: insights into the origin of methanogenesis, phototrophy, and the colonization of land. *BMC Evolutionary Biology,* **4**, 44.

Beal EJ, House CH, Orphan VJ (2009) Manganese- and iron-dependent marine methane oxidation. *Science,* **325**, 184-187.

Brandes JA (2009) Rapid and precise $\delta 13C$ measurement of dissolved inorganic carbon in natural waters using liquid chromatography coupled to an isotope□ratio mass spectrometer. *Limnology and Oceanography: Methods,* **7**, 730-739.

Caldwell SL, Laidler JR, Brewer EA, Eberly JO, Sandborgh SC, Colwell FS (2008) Anaerobic oxidation of methane: mechanisms, bioenergetics, and the ecology of associated microorganisms. *Environmental science & technology,* **42**, 6791-6799.

Caporaso JG, Lauber CL, Walters WA, Berg-Lyons D, Lozupone CA, Turnbaugh PJ, Fierer N, Knight R (2011) Global patterns of 16S rRNA diversity at a depth of millions of sequences per sample. *Proceedings of the National Academy of Sciences,* **108**, 4516-4522.

Craddock PR, Dauphas N (2011) Iron and carbon isotope evidence for microbial iron respiration throughout the Archean. *Earth and Planetary Science Letters,* **303**, 121-132.

Crowe S, Katsev S, Leslie K, Sturm A, Magen C, Nomosatryo S, Pack M, Kessler J, Reeburgh W, Roberts J (2011) The methane cycle in ferruginous Lake Matano. *Geobiology,* **9**, 61-78.

Crowe S, Roberts J, Weisener C, Fowle D (2007) Alteration of iron□rich lacustrine sediments by dissimilatory iron□reducing bacteria. *Geobiology,* **5**, 63-73.

Crowe SA, Jones C, Katsev S, Magen CD, O'neill AH, Sturm A, Canfield DE, Haffner GD, Mucci A, Sundby BR (2008a) Photoferrotrophs thrive in an Archean Ocean analogue. *Proceedings of the National Academy of Sciences,* **105**, 15938-15943.

Crowe SA, O'neill AH, Katsev S, Hehanussa P, Haffner GD, Sundby B, Mucci A, Fowle DA (2008b) The biogeochemistry of tropical lakes: A case study from Lake Matano, Indonesia. *Limnology Oceangraphy,* **53**, 319-331.

Edgar RC, Haas BJ, Clemente JC, Quince C, Knight R (2011) UCHIME improves sensitivity and speed of chimera detection. *Bioinformatics,* **27**, 2194-2200.

Egger M, Rasigraf O, Sapart CLJ, Jilbert T, Jetten MS, Ro☐Ckmann T, Van Der Veen C, Ba☐Nda☐ N, Kartal B, Ettwig KF (2015) Iron-mediated anaerobic oxidation of methane in brackish coastal sediments. *Environmental Science & Technology,* **49**, 277-283.

Farquhar J, Zerkle AL, Bekker A (2011) Geological constraints on the origin of oxygenic photosynthesis. *Photosynthesis Research,* **107**, 11-36.

Fournier GP, Gogarten JP (2008) Evolution of acetoclastic methanogenesis in *Methanosarcina* via horizontal gene transfer from cellulolytic *Clostridia. Journal of Bacteriology,* **190**, 1124-1127.

Fu L, Li S-W, Ding Z-W, Ding J, Lu Y-Z, Zeng RJ (2016) Iron reduction in the DAMO/*Shewanella oneidensis* MR-1 coculture system and the fate of Fe(II). *Water Research,* **88**, 808-815.

Hansel CM, Benner SG, Neiss J, Dohnalkova A, Kukkadapu RK, Fendorf S (2003) Secondary mineralization pathways induced by dissimilatory iron reduction of ferrihydrite under advective flow. *Geochimica et Cosmochimica Acta,* **67**, 2977-2992.

Hansen JW, Thamdrup B, Jørgensen BB (2000) Anoxic incubation of sediment in gas-tight plastic bags: a method for biogeochemical process studies. *Marine Ecology Progress Series,* **208**, 273-282.

Haqq-Misra JD, Domagal-Goldman SD, Kasting PJ, Kasting JF (2008) A revised, hazy methane greenhouse for the Archean Earth. *Astrobiology,* **8**, 1127-1137.

Hori T, Müller A, Igarashi Y, Conrad R, Friedrich MW (2010) Identification of iron-reducing microorganisms in anoxic rice paddy soil by 13C-acetate probing. *The ISME journal,* **4**, 267-278.

Jensen MM, Thamdrup B, Rysgaard S, Holmer M, Fossing H (2003) Rates and regulation of microbial iron reduction in sediments of the Baltic-North Sea transition. *Biogeochemistry,* **65**, 295-317.

Johnson CM, Beard BL, Roden EE (2008) The iron isotope fingerprints of redox and biogeochemical cycling in modern and ancient Earth. *Annual Reviews of Earth and Planetary Sciences,* **36**, 457-493.

Kappler A, Pasquero C, Konhauser KO, Newman DK (2005) Deposition of banded iron formations by anoxygenic phototrophic Fe(II)-oxidizing bacteria. *Geology,* **33**, 865-868.

Kashefi K, Holmes DE, Baross JA, Lovley DR (2003) Thermophily in the Geobacteraceae: Geothermobacter ehrlichii gen. nov., sp. nov., a Novel Thermophilic Member of the Geobacteraceae from the "Bag City" Hydrothermal Vent. *Applied and Environmental Microbiology,* **69**, 2985-2993.

Kasting JF (2005) Methane and climate during the Precambrian era. *Precambrian Research* **137**, 119-129.

501 Knoll AH, Bergmann KD, Strauss JV (2016) Life: the first two billion years. *Phil. Trans. R. Soc.*
502   *B,* **371**, 20150493.

503 Konhauser K, Newman D, Kappler A (2005) The potential significance of microbial Fe(III)
504   reduction during deposition of Precambrian banded iron formations. *Geobiology,* **3**, 167-
505   177.

506 Kostka JE, Luther GW (1994) Partitioning and speciation of solid phase iron in saltmarsh
507   sediments. *Geochemica Cosmochimica Acta,* **58**, 1701-1710.

508 Kostka JE, Roychoudhury A, Van Cappellen P (2002) Rates and controls of anaerobic microbial
509   respiration across spatial and temporal gradients in saltmarsh sediments.
510   *Biogeochemistry,* **60**, 49-76.

511 Kozich JJ, Westcott SL, Baxter NT, Highlander SK, Schloss PD (2013) Development of a dual-
512   index sequencing strategy and curation pipeline for analyzing amplicon sequence data on
513   the MiSeq Illumina sequencing platform. *Applied and environmental microbiology,* **79**,
514   5112-5120.

515 Lovley D, Phillips E (1986) Organic matter mineralization with reduction of ferric iron in
516   anaerobic sediments. *Applied and Environmental Microbiology,* **51**, 683-689.

517 Lovley DR, Goodwin S (1988) Hydrogen concentrations as an indicator of the predominant
518   terminal electron-accepting reactions in aquatic sediments. *Geochimica et Cosmochimica*
519   *Acta,* **52**, 2993-3003.

520 Lovley DR, Phillips EJ (1987) Competitive mechanisms for inhibition of sulfate reduction and
521   methane production in the zone of ferric iron reduction in sediments. *Applied and*
522   *Environmental Microbiology,* **53**, 2636-2641.

523 Niemann H, Steinle L, Blees J, Bussmann I, Treude T, Krause S, Elvert M, Lehmann MF (2015)
524   Toxic effects of lab-grade butyl rubber stoppers on aerobic methane oxidation. *Limnology*
525   *and Oceanography: Methods,* **13**, 40-52.

526 Noroi KA, Thamdrup B, Schubert CJ (2013) Anaerobic oxidation of methane in an iron-rich
527   Danish freshwater lake sediment. *Limnology and oceanography,* **58**, 546-554.

528 Pavlov AA, Kasting JF, Brown LL, Rages KA, Freedman R (2000) Greenhouse warming by
529   CH4 in the atmosphere of early Earth. *Journal of Geophysical Research: Planets,* **105**,
530   11981-11990.

531 Posth NR, Konhauser KO, Kappler A (2013) Microbiological processes in banded iron formation
532   deposition. *Sedimentology,* **60**, 1733-1754.

533 Poulton SW, Canfield DE (2005) Development of a sequential extraction procedure for iron:
534   implications for iron partitioning in continentally derived particulates. *Chemical Geology,*
535   **214**, 209-221.

536 Poulton SW, Canfield DE (2011) Ferruginous conditions: a dominant feature of the ocean
537   through Earth's history. *Elements,* **7**, 107-112.

538 Riedinger N, Formolo M, Lyons T, Henkel S, Beck A, Kasten S (2014) An inorganic
539   geochemical argument for coupled anaerobic oxidation of methane and iron reduction in
540   marine sediments. *Geobiology,* **12**, 172-181.

541 Roden EE, Wetzel RG (1996) Organic carbon oxidation and suppression of methane production
542   by microbial Fe (III) oxide reduction in vegetated and unvegetated freshwater wetland
543   sediments. *Limnology and Oceanography,* **41**, 1733-1748.

544 Roden EE, Wetzel RG (2002) Kinetics of microbial Fe (III) oxide reduction in freshwater
545   wetland sediments. *Limnology and Oceanography,* **47**, 198-211.

546 Rooze J, Egger M, Tsandev I, Slomp CP (2016) Iron☐dependent anaerobic oxidation of methane
547   in coastal surface sediments: Potential controls and impact. *Limnology and*
548   *Oceanography*.

549 Rotaru A-E, Shrestha PM, Liu F, Shrestha M, Shrestha D, Embree M, Zengler K, Wardman C,
550   Nevina KP, Lovley DR (2014) A new model for electron flow during anaerobic
551   digestion: direct interspecies electron transfer to Methanosaeta for the reduction of
552   carbon dioxide to methane. *Energy & Environmental Science,* **7**, 408-415.

553 Scheller S, Yi H, Chadwick GL, Mcglynn SE, Orphan VJ (2016) Artificial electron acceptors
554   decouple archaeal methane oxidation from sulfate reduction. *Science,* **351**, 703-707.

555 Schloss PD, Westcott SL, Ryabin T, Hall JR, Hartmann M, Hollister EB, Lesniewski RA,
556   Oakley BB, Parks DH, Robinson CJ (2009) Introducing mothur: open-source, platform-
557   independent, community-supported software for describing and comparing microbial
558   communities. *Applied and environmental microbiology,* **75**, 7537-7541.

559 Segarra KEA, Comerford C, Slaughter J, Joye SB (2013) Impact of electron acceptor availability
560   on the anaerobic oxidation of methane in coastal freshwater and brackish wetland
561   sediments. *Geochimica et Cosmochimica Acta,* **115**, 15-30.

562 Sivan O, Adler M, Pearson A, Gelman F, Bar-Or I, John SG, Eckert W (2011) Geochemical
563   evidence for iron-mediated anaerobic oxidation of methane. *Limnology and*
564   *Oceanography,* **56**, 1536-1544.

565 Sivan O, Antler G, Turchyn AV, Marlow JJ, Orphan VJ (2014) Iron oxides stimulate sulfate-
566   driven anaerobic methane oxidation in seeps. *Proceedings of the National Academy of*
567   *Sciences,* **111**, 4139-4147.

568 Sivan O, Shusta SS, Valentine DL (2016) Methanogens rapidly transition from methane
569   production to iron reduction. *Geobiology,* **DOI: 10.1111/gbi.12172**.

570 Stolz JF, Ellis DJ, Blum JS, Ahmann D, Lovley DR, Oremland RS (1999) Note: Sulfurospirillum
571   barnesii sp. nov. and Sulfurospirillum arsenophilum sp. nov., new members of the

572   Sulfurospirillum clade of the ε-Proteobacteria. *International Journal of Systematic and*
573   *Evolutionary Microbiology,* **49**, 1177-1180.

574 Stookey LL (1970) Ferrozine---a new spectrophotometric reagent for iron. *Analytical Chemistry,*
575   **42**, 779-781.

576 Sturm A, Fowle DA, Jones C, Leslie KL, Nomosatryo S, Henny C, Canfield DE, Crowe S
577   (2015) Rates and pathways of methane oxidation in ferruginous Lake Matano, Indonesia.
578   *Biogeosciences Discussions,* **12**, 1-34.

579 Ueno Y, Yamada K, Yoshida N, Maruyama S, Isozaki Y (2006) Evidence from fluid inclusions
580   for microbial methanogenesis in the early Archaean era. *Nature,* **440**, 516-519.

581 Vargas M, Kashefi K, Blunt-Harris EL, Lovley DR (1998) Microbiological evidence for Fe(III)
582   reduction on early Earth. *Nature,* **395**, 65-67.

583 Zavarzina DG, Sokolova TG, Tourova TP, Chernyh NA, Kostrikina NA, Bonch-Osmolovskaya
584   EA (2007) Thermincola ferriacetica sp. nov., a new anaerobic, thermophilic, facultatively
585   chemolithoautotrophic bacterium capable of dissimilatory Fe(III) reduction.
586   *Extremophiles,* **11**, 1-7.

587 Zehnder AJ, Brock TD (1980) Anaerobic methane oxidation: occurrence and ecology. *Applied*
588   *and Environmental Microbiology,* **39**, 194-204.

589 Zhou S, Xu J, Yang G, Zhuang L (2014) Methanogenesis affected by the co-occurrence of iron
590   (III) oxides and humic substances. *FEMS Microbiology Ecology,* **88**, 107-120.

591

592

593

594

595

596

597

598

599   **Figure Captions**

600   **Figure 1. HCl-extractable Fe^{2+} for sediment enrichments with (a) ferrihydrite and (b)**

601   **goethite over 497 days**. Timeline at top shows transfer dates and dilution ratios. "A" represents

602   days that controls were autoclaved. Red and black symbols represent treatments with and without

603   CH_4, respectively. White symbols represent autoclaved controls. All treatments were run in

604   duplicate (circle and triangle symbols). Tertiary enrichments are magnified as inset. Photos

605   depict $2°$ and $3°$ enrichment bottles on day 497 with evidence for magnetic mineral formation in

606   live treatments amended with ferrihydrite.
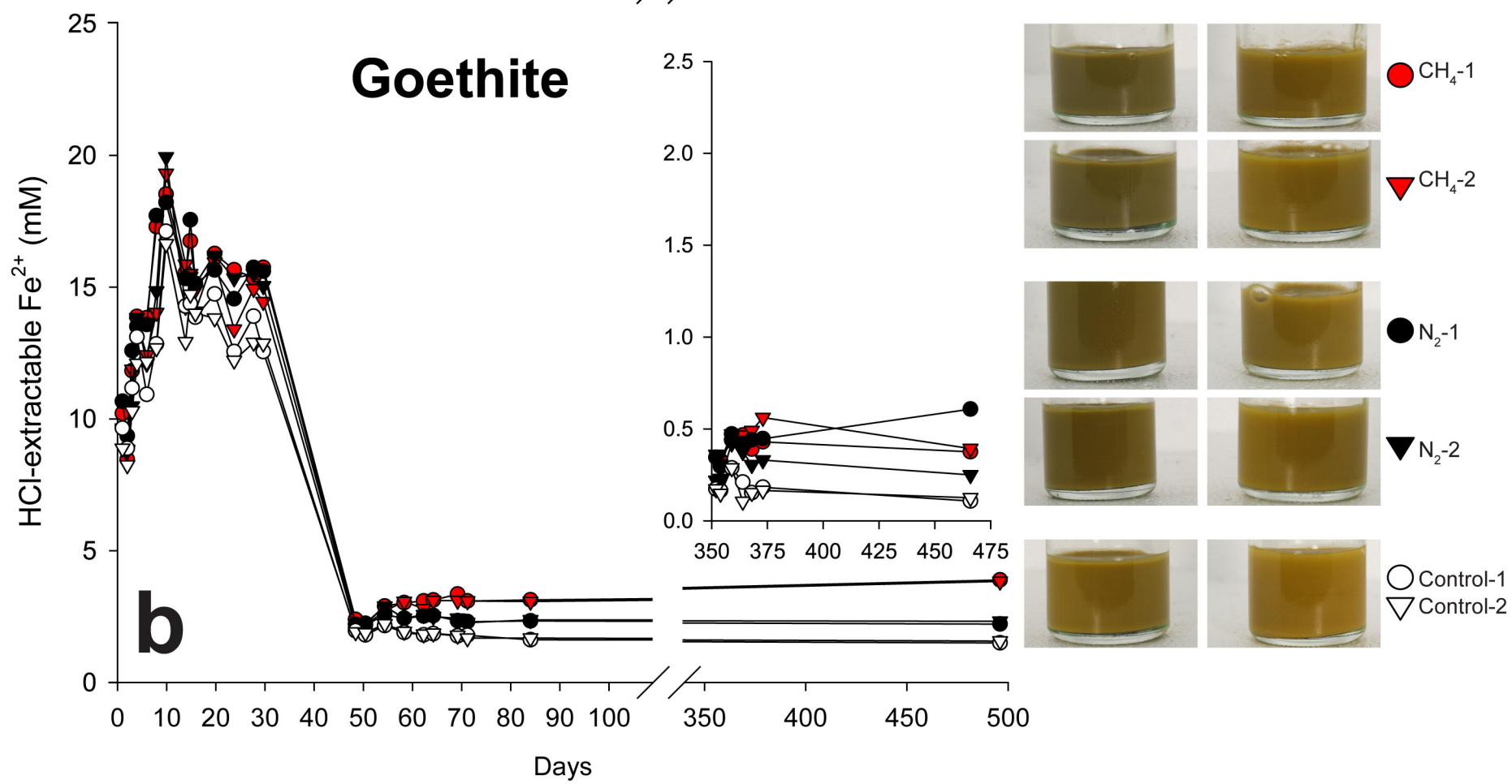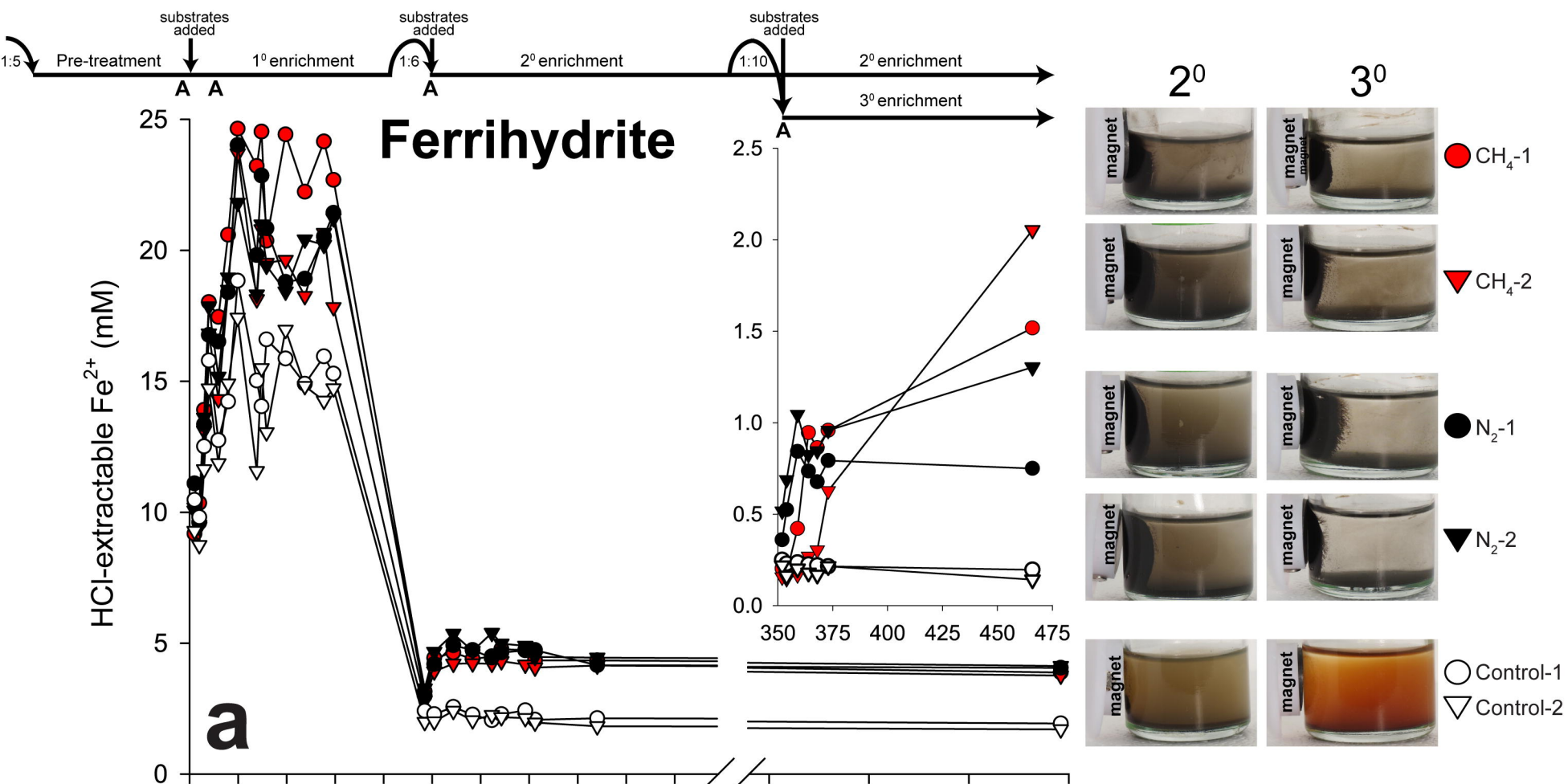
607   **Figure 2. Accumulation of CH_4 in the headspace of sediment enrichments.** Timeline at top

608   shows transfer dates and dilution ratios. Solid and dotted lines represent ferrihydrite and goethite

609   treatments, respectively. All treatments were run in duplicate (circle and triangle symbols).
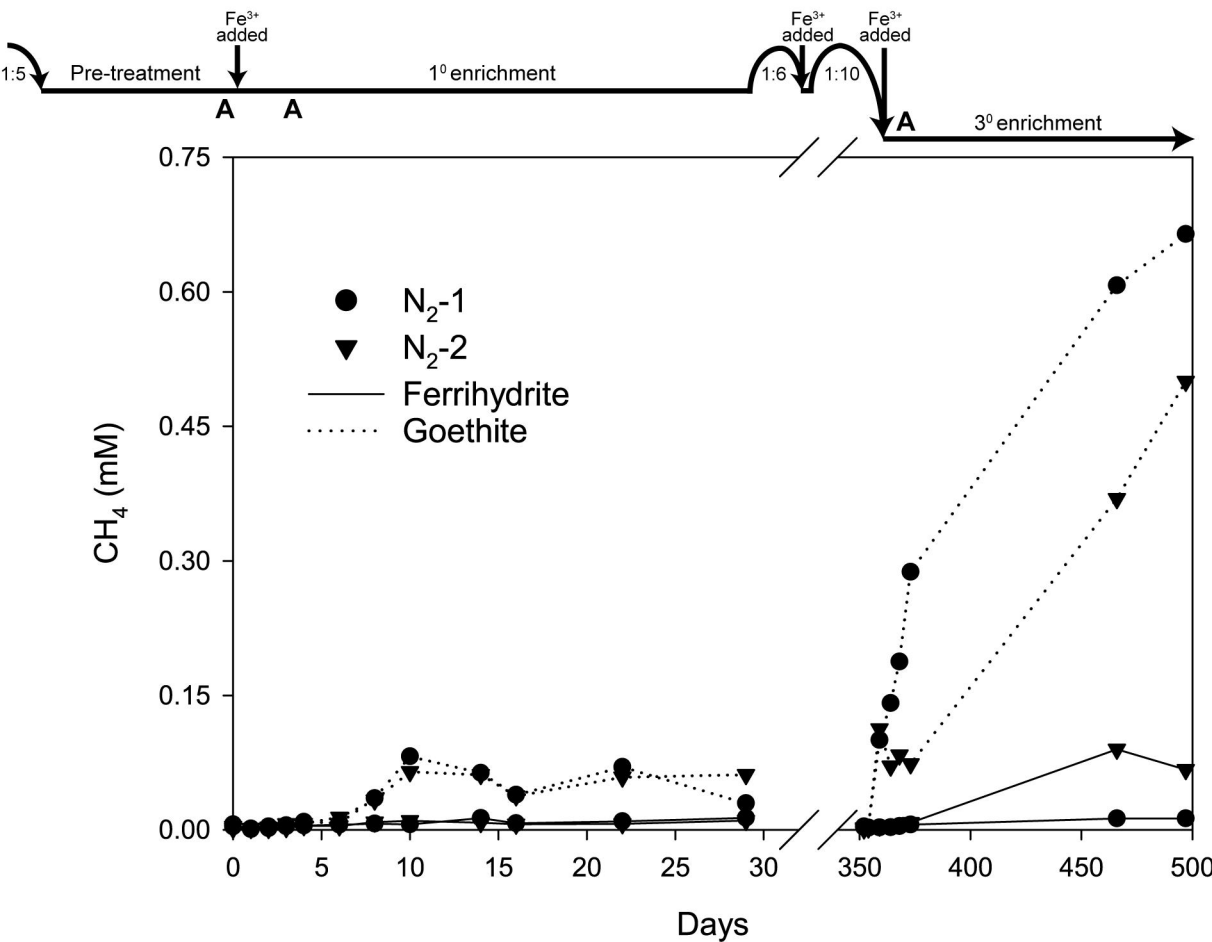
610   Original headspace was 100% N_2.

611   **Figure 3. Dissolved inorganic carbon (DIC) isotopic composition and concentration for**

612   **sediment enrichments amended with $^{13}CH_4$ and either (a,c) ferrihydrite or (b,d) goethite.**

613   Timeline at top shows transfer dates and dilution ratios. "A" represents days that controls were

614   autoclaved. Red and white symbols represent live treatments and autoclaved controls,

615   respectively. Errors bars represent standard deviation of triplicate measurements. Calculated

616   methane oxidation rates for the $1°$ enrichment were 1.7 and 1.1 μM CH_4 d^{-1} ferrihydrite bottles 1

617   and 2, respectively and 0.2 and 0.8 μM CH_4 d^{-1} for goethite bottles 1 and 2, respectively. Isotopic

618   data are not plotted for DIC concentrations 0.5 mM. Rate calculations were not possible for the

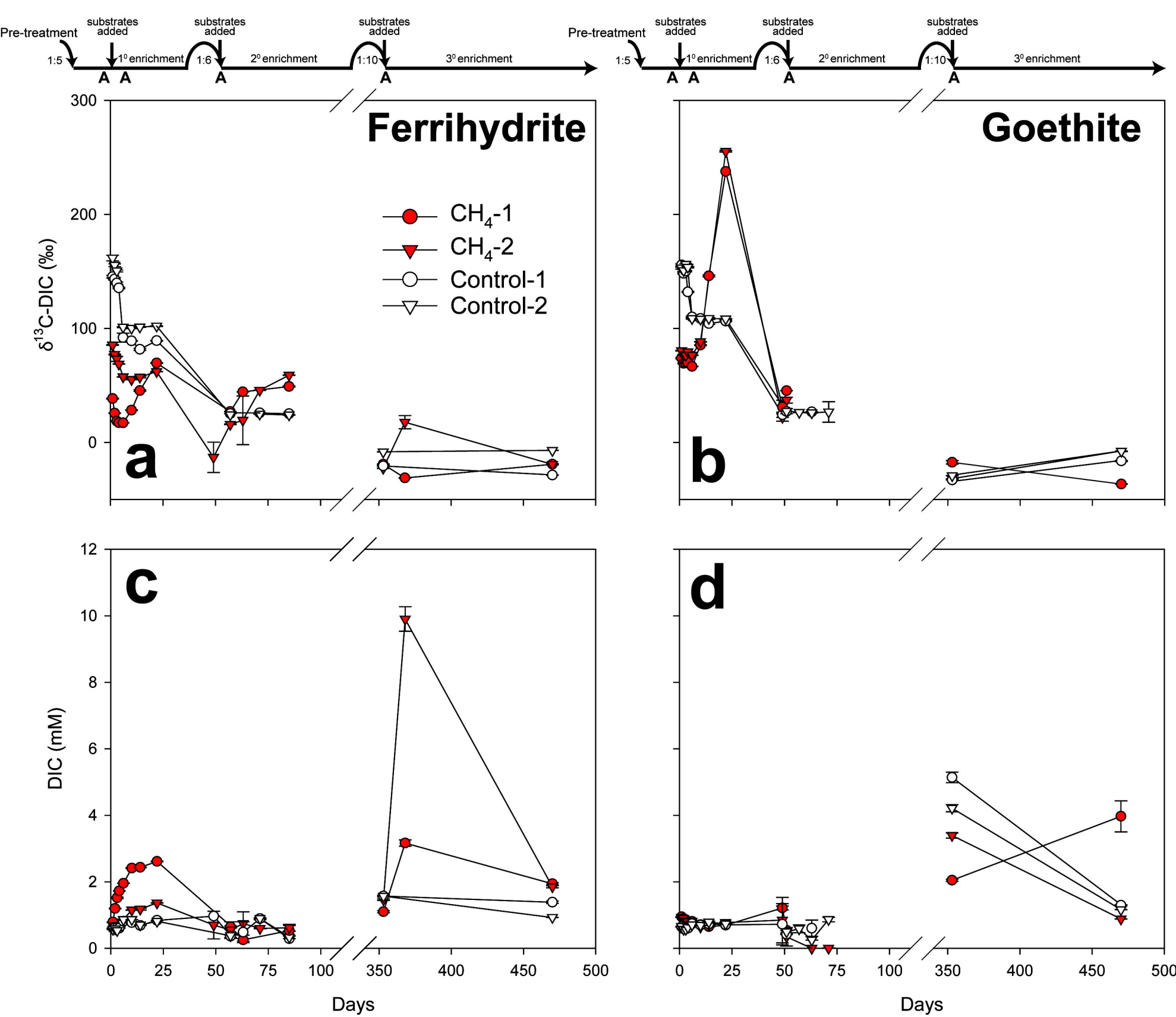619 $2°$ enrichment due to low/variable DIC.

26

620 **Figure 4. 16S rRNA gene diversity and phylogenetic diversity for inoculum and sediment**

621 **enrichments amended with (a) ferrihydrite and (b) goethite.** Samples were taken on day 15

622 (1° enrichment), 72 (2° enrichment) and 469 (3° enrichment). Red and black symbols represent

623 treatments with and without CH_4, respectively. Gray diamonds represent inoculum samples. All

624 treatments were run in duplicate (circle and triangle symbols). Species richness, phylogenetic

625 diversity, and species evenness for the sediment inoculum and enrichments normalized to 4000

626 sequences per sample are shown to the right of barcharts.

627 **Figure 5. Rates of HCl-extractable Fe^{3+} reduction rates vs. CH_4 production (black symbols)**

628 **or CH_4 oxidation (red symbols).** Autoclaved controls are white circles. "F" indicates

629 ferrihydrite and "G" indicates goethite. The red line indicates the line for the predicted ratio of 1

630 mol CH_4 oxidized per 8 mol Fe^{3+} reduced. Tertiary enrichments are magnified as inset.

631

Pre-treatment — 1^0 enrichment — 2^0 enrichment — 2^0 enrichment / 3^0 enrichment

substrates added

1:5 · A A · 1:6 · A · 1:10 · A

2^0 3^0

Ferrihydrite

HCl-extractable Fe^{2+} (mM)

a

● CH$_4$-1
▼ CH$_4$-2
● N$_2$-1
▼ N$_2$-2
○ Control-1
▽ Control-2

Goethite

HCl-extractable Fe^{2+} (mM)

b

● CH$_4$-1
▼ CH$_4$-2
● N$_2$-1
▼ N$_2$-2
○ Control-1
▽ Control-2

Days

Pre-treatment substrates added substrates added substrates added

1:5 1^0 enrichment 1:6 2^0 enrichment 1:10 3^0 enrichment

A A   A   A

Pre-treatment substrates added substrates added substrates added

1:5 1^0 enrichment 1:6 2^0 enrichment 1:10 3^0 enrichment

A A   A   A

Ferrihydrite

Goethite

δ^{13}C-DIC (‰)

300

200

100

0

CH$_4$-1
CH$_4$-2
Control-1
Control-2

a

b

DIC (mM)

12

10

8

6

4

2

0

c

d

Days

Days

0 25 50 75 100 350 400 450 500

0 25 50 75 100 350 400 450 500

Ferrihydrite

Goethite